



LAWRENCE  
LIVERMORE  
NATIONAL  
LABORATORY

# Mechanical Damage, Ignition, and Burn: Experiment, Model Development, and Computer Simulations to Study High-Explosive Violent Response (HEVR)

J. E. Reaugh, A. G. Jones

January 26, 2010

14th International Detonation Symposium  
Coeur d'Alene, ID, United States  
April 11, 2010 through April 16, 2010

## **Disclaimer**

---

This document was prepared as an account of work sponsored by an agency of the United States government. Neither the United States government nor Lawrence Livermore National Security, LLC, nor any of their employees makes any warranty, expressed or implied, or assumes any legal liability or responsibility for the accuracy, completeness, or usefulness of any information, apparatus, product, or process disclosed, or represents that its use would not infringe privately owned rights. Reference herein to any specific commercial product, process, or service by trade name, trademark, manufacturer, or otherwise does not necessarily constitute or imply its endorsement, recommendation, or favoring by the United States government or Lawrence Livermore National Security, LLC. The views and opinions of authors expressed herein do not necessarily state or reflect those of the United States government or Lawrence Livermore National Security, LLC, and shall not be used for advertising or product endorsement purposes.

# Mechanical Damage, Ignition, and Burn: Experiment, Model Development, and Computer Simulations to Study High-Explosive Violent Response (HEVR)

John E. Reaugh<sup>a</sup> and Andrew G. Jones<sup>b</sup>

<sup>a</sup>Lawrence Livermore National Laboratory, Livermore, CA 94551 USA

<sup>b</sup>Atomic Weapons Establishment, Reading, Berkshire, RG7 4PR, UK

**Abstract.** Low-velocity impact of explosives and propellants can, in some circumstances, lead to a more-or-less violent release of some of the chemical energy (HEVR) without developing into a detonation. Research test vehicles, such as the Steven and spigot tests, and results from other tests on explosives have been interpreted by expert judgment to assess the likelihood of a violent reaction in response to industrial or transportation accidents. We are fielding tests and developing models to use in computer simulations of test vehicles and postulated accident scenarios. Combining the results of experiments and simulations helps inform expert judgment.

---

## Introduction

Working with or transporting explosive assemblies safely requires procedures that account for the dangers posed by the specific explosive formulation, and the potential hazards associated with ordinary industrial processes, including drops, falls, and road accidents. In the past, safety tests were developed to serve as a guide to handling procedures.<sup>1</sup> The small-scale drop hammer test<sup>2,3</sup> was used to screen new materials into categories familiar to explosive handlers: TATB-like, TNT-like, CompB-like, PETN-like, or NG-like. The oblique impact<sup>4,5</sup> or skid test explored the interaction of a large explosive billet skidding on an industrial floor. Such tests were used to evaluate both the hazard posed by the drop of a large quantity of a specific explosive, and the relative desirability of specific floor coverings. Somewhat higher impact velocities were used in the Susan test,<sup>6</sup> Steven test,<sup>7-9</sup> and spigot test,<sup>10</sup> all of which subject an explosive to a locally crushing impact.

For all of these tests, the velocity of impact is well below that required to run to detonation in the volume of material tested. For many of the tests,

the pressure developed upon impact is not a shock, but rather an adiabatic pressure rise. In most of the tests, there is a substantial residue of unreacted explosive in the test area. Inferring the danger to people and structures by a postulated accident has required the results of a battery of tests as interpreted by expert judgment to assess the violence of the reaction.

We are developing a model for use in computer simulations. We simulate a battery of tests, in order to set the value of parameters in the model, and then also simulate postulated accidents. In this we help inform expert judgment of the similarities and differences in the insult experienced by the explosive, so that the degree of violence of the reaction might be more accurately assessed. In addition we use the model to help design new tests, which may more accurately reproduce the insult caused by a postulated accident.

## Processes Leading to Violent Reaction

If an energetic material is subjected to a mechanical insult, such as a drop or an impact that is well below the threshold for detonation, a volume

of explosive near the impact area can be damaged. The damage is manifest as surface area, through the creation of cracks and fragments, and as porosity, through the separation of crack faces and isolation of the fragments. As the kinetic energy and power of the insult increases, the degree of damage and the volume of damage both increase. Upon a localized ignition, the flame spreads to envelop the damaged volume. Open porosity permits a flame to spread easily and so ignite the surface area that was created. The locally increased surface area causes a local increase in the mass-burning rate. The pressure rises at an accelerated rate until neither mechanical strength nor inertial confinement of the surrounding material successfully contains the pressure. The confining structure begins to expand. This reduces the pressure and may even extinguish the flame. Both the mass of explosive involved and the rate at which the gas is produced contribute to each of several different measures of violence. Such measures include damage to the confinement, the velocity and fragment size distributions from what was the confinement, and air blast. Figure 1 illustrates the interaction of the various processes described above.

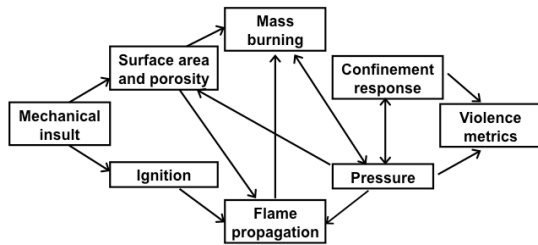


Fig. 1. Following a mechanical insult, interacting processes lead to disruption of the confinement, which is quantified by a violence metric.

Our model of these interacting processes comprises several interacting elements. The constitutive model describes the strength of the explosive. In our simulations, the plastic strain and strain localization are strongly influenced by the constitutive model. The development of specific surface area and porosity are intimately connected with the constitutive model. An ignition criterion is used to assess the time and location of the start of burning, based on the local field variables. An ignition front then propagates through the dam-

aged material. The local mass rate of burning is based on the laminar burn speed (surface flame burning into the fragments), which is measured as a function of pressure, and the calculated specific surface area. Pressure is determined by the equations of state of the solid unburned explosive and the gas products, along with pressure equilibrium but not temperature equilibrium. The progressive failure of the confinement depends on the structural properties of the surrounding structure. The model is intended for implementation in a general-purpose simulation program (hydrocode) that solves the partial differential equations for the conservation of mass, momentum, and energy in conjunction with equations of state and strength. Details of the model equations and algorithms not provided here are available in four LLNL reports.<sup>11-14</sup>

### Constitutive Model

In our early implementation of the model, we used constant vonMises strength for the explosive. The consequence of using constant strength was that strains localized to such an extent that the criteria for specific surface area and ignition were inversely dependent on the computational mesh size. In principle, one can use a criterion that is the product of nominal (or actual, changing) computational mesh and the criterion. Rather than that, we decided to use a pressure and strain-rate dependent geomechanics model developed for concrete.<sup>15</sup> We note that this sort of model is also used by Gruau *et al.*<sup>16</sup> for their calculations of Steven tests.

The explosive we are studying, in common with most materials with pressure-dependent flow stress, has tensile strength that is much lower than the compressive strength. Simulations of such materials that feature tensile failure are severely mesh sensitive. Our model has been implemented (and the examples described here simulated) with LS-DYNA<sup>17</sup>. When simulating the frangibility test,<sup>18</sup> which is a Taylor impact on a relatively rigid steel plate, tensile stress does not develop normal to the impact interface, and extra tensile failure does not occur. In Eulerian implementations, the interface will in general be a mixed cell with non-zero tensile strength, which can lead to mesh-sensitive failure unless special care is taken.

## Models for Porosity, Specific Surface Area, and Ignition

When an associated flow rule, or a flow-rule normal to a surface with reduced pressure dependence is used, the plastic strain rates include a volumetric component that we use to increase the local porosity of damaged material.

We use a simplification of the model we developed for propellants,<sup>19</sup> which was calibrated to frangibility test results, to calculate the specific surface area of the UK explosive we are studying. In the simplified model, the specific surface area is proportional to the plastic strain, reduced by a plastic strain threshold that is required to be achieved before any fracture happens.

Ignition is critical to analyzing whether a specific mechanical insult leads to HEVR. Some have used modified shock-to-detonation models for HEVR response.<sup>20</sup> There are theoretical objections to this approach for HEVR and pragmatic ones as well. The main theoretical objection is that HEVR is generally not a detonation. Substantial quantities of unreacted explosive are found scattered about the test area even when a violent event is recorded on blast gauges. The steel confinement is in much larger pieces than is found after a deliberate detonation. In addition, the steel lacks the characteristic appearance that results when it has been adjacent to a detonation. The main pragmatic objection is that the pressure or compressive stress calculated at the HEVR threshold is substantially different in different test geometries.

For our ignition model, we rely on the observation that in low-speed impacts, such as the Susan, Steven, skid, and spigot tests, ignition is accompanied by significant shear deformation. We do not identify whether the localization mechanism is crystal twinning, continuum shear bands, friction, grain-to-grain interference, explosive-grit interaction, or other possibility. (In the Steven test, there is no grit.) Instead, we use properties of the stress tensor to identify where shear deformation is occurring. Specifically, if the principal stress deviators are ordered algebraically, the intermediate principal stress deviator is zero when the plastic strain rate corresponds to pure shear. Our ignition term is a weighted integral of the plastic strain rate with pure shear deformation and high normal stress on the plane of maximum shear receiving the most weight.

## Calculation of Pressure

In most studies of the Deflagration to Detonation Transition, DDT, the stress in the mixture is partitioned into the gas pressure, the solid pressure, and the stress in the solid particles due to stress bridging in the skeleton.<sup>21,22</sup> In the rock and soil mechanics literature, the matrix pressure in the solid skeleton that is greater than the pressure in the intervening fluid (water) is called the effective pressure. The shear resistance of the skeleton depends on the effective stress. If the pressure in the fluid equals or exceeds the pressure in the skeleton, the particles lose contact, and the shear resistance is nil. The overall resistance to consolidation offered by the matrix is a modest multiplier of the shear strength of the full density material until the last stages of densification, when the multiplier can reach 10 or more.

Temperature is not equilibrated. The flame front, which is the gas and solid interface, is thin relative to the fragment dimension. As a result, most of the solid is at the initial temperature, not the temperature of the hot gas, which can reach 3000K. To determine the energy partition between gas and solid, we use the method of isochoric burn.<sup>23</sup> In that method, the solid is on its adiabat and the gas gets the energy that is left over.

We use the JWL form<sup>24</sup> for the solid equation of state, and a constant specific heat of the solid for calculating what is at best an advisory temperature.

We developed an equation of state table for the gas products using Cheetah.<sup>25,26</sup> The density range of the table is  $10^{-4}$  to 3.5 g/cc, and the temperature range is 270 to 40,000K. (At temperatures of about 10,000K and above, ionization effects in the gas begin to play a role.) Interpolation in the table is linear in the logarithm of density, linear in temperature and energy density, and logarithmic in pressure.

An important feature of the resistance of the matrix is its irreversibility. The matrix is an assembly of particles touching on some of their surfaces. Compression of that matrix is accompanied by a rearrangement of the particles that produces an irreversible compaction, and an increasing resistance to further consolidation. An unloading-reloading path that has a higher modulus than the consolidation limit provides irreversibility. We developed a model<sup>27</sup> that describes this irreversible

consolidation and includes explicitly the reference state porosity. If the burning process reduces the mass from the available surfaces of the particles, and they do not rearrange themselves, then the porosity (the fraction of the total volume not occupied by solid material) increases with the extent of reaction,  $\lambda$ .

$$\varphi = \phi_g = \lambda \frac{v_g}{v_0} = 1 - \phi_s = 1 - \frac{v_s(1-\lambda)}{v_0}. \quad (1)$$

where  $\varphi$  is the porosity,  $\phi_{s,g}$  the volume fractions of solid or gas,  $v_{s,g}$  are the specific volumes of the solid or gas at the initial pressure, and  $v_0$  is the initial specific volume.

At some porosity, on the order of 40%, (relative volume  $V \approx 1.6$ ) the matrix can no longer support any stress because the particles no longer touch, and the matrix pressure is considered zero. Since, in our view, the damaged material is broken, we do not permit the matrix stress to be tensile. A history variable is set when the matrix over-expands, so that recompression is not resisted until the previous density at zero pressure is re-achieved. This is consistent with the view that the expanding assembly does not rearrange itself to maintain contact between the particles, but rather separates as isolated fragments. It should be noted that the pressure, calculated in this model<sup>27</sup> is that appropriate for the macroscopic stress acting on a plane. This macroscopic matrix pressure,  $P_{mm}$ , is given by

$$P_{mm} = \phi_s P_m \quad (2)$$

where  $P_m$  is the matrix stress.

The pressure of the mixture is given by

$$P = \phi_s P_s + (1 - \phi_s) P_g, \quad (3)$$

where  $P_s$  is the solid pressure, and  $P_g$  is the gas pressure. Pressure equilibrium requires that

$$P_s = P_g + P_m. \quad (4)$$

### Calculation of Ignition Propagation and Burning

Once ignition occurs, hot gas from the ignition site expands through the surrounding porous, damaged, but unlit explosive. The speed of propagation cannot exceed the sound speed of the hot gas, which is about 1 km/s. The criterion for ignition will require the hot gas to be in contact with the solid for a long enough time that the surface can be raised to the ignition temperature. Since the prod-

uct species in the gas can react with the solid<sup>28</sup> the actual ignition temperature may be less than the ignition temperature when heated by a hot but inert gas. For our initial calculations, we assume that both the tortuosity of the path and the delay time can be represented by an effective slow-down of the propagation velocity. Our baseline calculations use the value 300 m/s for the velocity of ignition spread.

Although the velocity of ignition spread is subsonic, we have assumed for simplicity that the time of ignition can be calculated from the geometry at the time of ignition. If an element subsequently exceeds the ignition limit value, the element ignites then, rather than waiting for the arrival of an ignition front.

The use of a constant propagation velocity is an extreme simplification. Multi-phase, multi-velocity simulations show that the propagation of an ignition front depends on the hot gas flow, which in turn depends on pressure, porosity, and channel size. Such simulations, coupled with experiments (to be defined) would be useful in modifying our simplification.

The final step is to update the extent of reaction at constant volume. The total energy remains the same, since, in our calculations, each constituent has its own energy of formation. The change in the extent of reaction for each computational element is given by

$$\frac{d\lambda}{dt} = \frac{S}{V} (1-\lambda)^{2/3} v_f \left[ \frac{\max(p, 0.1 \text{ MPa})}{p_0} \right]^n \quad (5)$$

where  $p_0 = 1 \text{ GPa}$ ,  $v_f = 1 \text{ m/s}$ , and  $n = 1$ , as described.<sup>11</sup>  $S/V$  is the local surface-to-volume ratio.

### Applications to a UK Explosive

The UK explosive we are studying is an HMX (1,3,5,7-tetranitro-1,3,5,7-tetraazacyclooctane) explosive, which is 91% by weight HMX and 9% binder-plasticizer, NC/DNEB/TNEB, which has a glass-transition temperature of 210° K. Tests performed on this material include tests of mechanical strength, as well as tests to determine ignition.

### Constitutive Model Calibration

We fit the constitutive model parameters to Split Hopkinson Pressure Bar (SHPB), modest rate uniaxial compression tests<sup>29,30</sup> and also quasi-static

triax tests<sup>31</sup>. The fit to the peak stress of the SHPB results uses the following functional form for the rate dependence, R

$$R = \left( 1 + \frac{\dot{\epsilon}_p}{\dot{\epsilon}_0 \exp[\alpha(T - T_0)]} \right)^{ep} \quad (6)$$

where  $\dot{\epsilon}_0$  is  $5.6 \text{ sec}^{-1}$ ,  $\alpha$  is 0.184 and  $ep$  is 0.14. The correlation of the Cavendish Lab data for peak stress and this functional form is shown in Figure 2. The fit to triax test data is shown in Figure 3.

### Experimental Test Vehicles and Results

The AWE Steven test comprises of a 70 mm diameter by 12.7 mm thick explosive disc with a 10 mm (radial) thick PTFE ring surrounding it. These are located inside a steel base unit, which provides a high level of confinement both radially and to the rear of the explosive. A 3 mm thick steel cover plate is located on top of the target providing full confinement to the explosive sample. The cover plate is secured to the base unit by a steel strong ring which bolts to the target stand plate. A 1.6 kg round nosed 50 mm diameter cylindrical steel projectile is fired at the centre of the cover plate of the target vehicle from a gas gun, Figure 4. The impact velocity of the projectile is varied in order to determine the threshold for reaction of the explosive being tested.

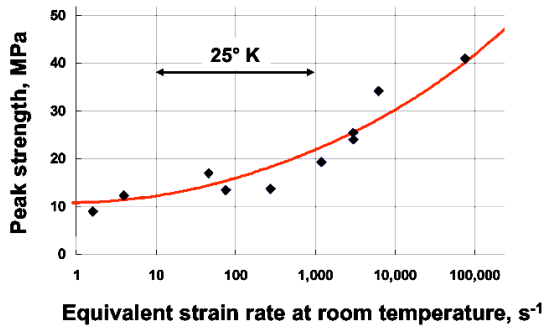


Fig. 2. Model fit (curve) to peak strength as a function of equivalent room-temperature strain-rate. The temperature shift is 12.5 K per decade.

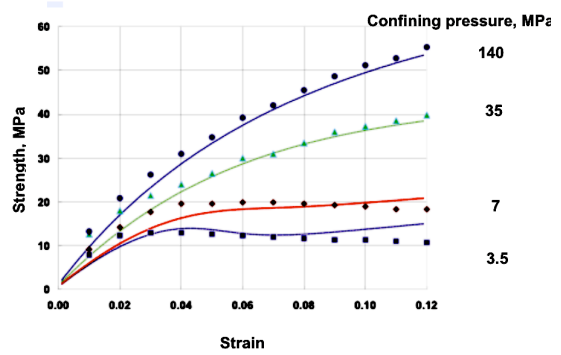


Fig. 3. Model fit (curves) to triax tests at various confining pressures (symbols)

The impact reaction threshold speed for the HMX-based explosive under consideration is between 62 and 64 m/s when impacted by the round nosed projectile in the AWE Steven test. Impacts at speeds lower than the threshold value leave dents in the cover plate and HE, Figures 5, 6.

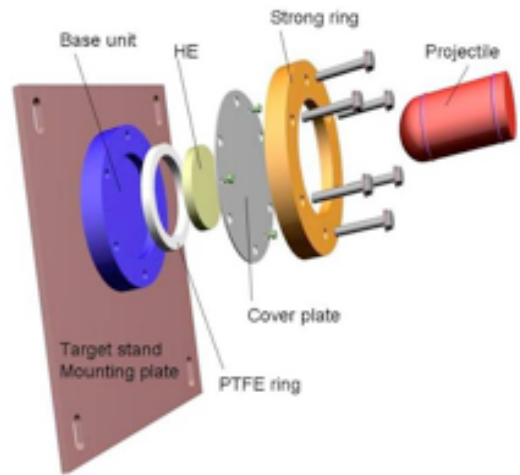


Fig. 4. Schematic of AWE Steven Test vehicle and projectile.



Fig. 5. Residual dent in the cover plate after an impact of 62.5 m/s that did not ignite.

Impacts at speeds higher than the reaction threshold produce violent reactions that partially consume the explosive and cause failure of the bolts securing the cover plate over the explosive test sample, relieving confinement. Figure 7 shows the unburned explosive left over after an impact of 74 m/s.



Fig. 6. Residual dent in the HE after an impact of 62.5 m/s that did not ignite.



Fig. 7. HE remnants after an impact at 74 m/s that did ignite. Of the original 89-gram charge, 55 grams were recovered.

#### Simulations of the Dent in the AWE Steven Test

We performed a series of simulations with LS DYNA that varied several experimental parameters to determine the depth of the dent at 70 m/s. This velocity is the lowest experimental velocity for which reaction occurs. In these simulations, however, we suppressed ignition and subsequent burning. We estimated what the measured dent in the absence of ignition would be by extrapolation. We used the calculated increase of dent depth with velocity to extrapolate the dent measured in the test at the highest velocity for which no ignition was observed. In our simulations, the dent is taken as the difference between the displacement of the top of the cover plate under the strong ring and the top of the cover plate on the axis of symmetry. The coefficient of friction between explosive and steel, and explosive and PTFE has been measured<sup>32</sup> to be about 0.4 for both LX-04, an HMX-based explosive developed at LLNL, and for an explosive mock at room temperature. The coefficient drops to half that value at 100° C. We observe that the depth of dent decreases monotonically with the assumed friction coefficient, as shown in Table 1. The dent depth increases when the strengths of any of the components is reduced. For these axisymmetric simulations, the elements in the steel and PTFE were approximately 1 mm square. The mesh in the HE was 0.33 mm in the radial direction and

0.6 mm in the axial direction. As the deformation under the projectile becomes severe, the mesh described more easily accommodates the resulting deformation without mesh tangling. The calculational results with nominal values after the projectile begins to rebound are shown in Figure 8.

Table 1. Calculated dent depth for AWE Steven test at 70 m/s. Dent with \* used PTFE strength of 0.001 GPa instead of 0.1 GPa. The extrapolated experimental dent at this velocity is 12 mm.

| Friction coefficient | Steel strength, GPa | HE max strength, GPa | Dent, mm |
|----------------------|---------------------|----------------------|----------|
| 0.05                 | 0.5                 | 0.3                  | 13.1     |
| 0.2                  | 0.5                 | 0.3                  | 11.4     |
| 0.4                  | 0.5                 | 0.3                  | 10.3     |
| 0.6                  | 0.5                 | 0.3                  | 9.8      |
| 0.4                  | 0.3                 | 0.3                  | 10.8     |
| 0.4                  | 0.5                 | 0.3                  | 12.1*    |
| 0.4                  | 0.5                 | 0.15                 | 11.0     |

We performed additional simulations where the mesh in the HE was altered, with the mesh in the surrounding steel and PTFE remaining the same. With the same aspect ratio, we varied the radial mesh from 0.1 to 0.67 mm. The dent calculated with the nominal values was the same in all cases.

#### Calculation of the Ignition Variable and Specific Surface Area

The maximum calculated ignition variable is seen to vary dramatically with the assumed coefficient of friction and the strength of materials in the test fixture, as is displayed in Table 2. The location of the maximum ignition parameter is in the HE very near the thick backing plate at a radial distance of about half the projectile radius. The mesh refinement study showed that the ignition parameter is dependent on mesh size, given by

$$\text{Ign} = 340 \exp(-1.59 \Delta r). \quad (7)$$

The calculated specific surface area is a maximum near the point of ignition, but is also large near the axis of symmetry, where the plastic strain is developed in triaxial compression rather than shear. The peak value is also exponentially dependent on mesh size.

$$\frac{S}{V} = 33 \exp(-1.11 \Delta r) \text{ mm}^{-1} \quad (8)$$

A sphere with 180- $\mu\text{m}$  diameter (or a cube of that dimension) has the specific surface area 33  $\text{mm}^{-1}$ .

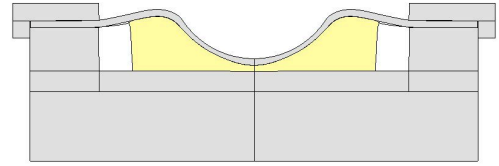


Fig. 8. Calculated dent in AWE Steven test at 70 m/s for nominal properties. The central HE disk (yellow) is surrounded by a PTFE ring (white) enclosed in steel.

Table 2. Calculated maximum ignition variable in AWE Steven test at 70 m/s. Value with \* used PTFE strength of 0.001 GPa.

| Friction coefficient | Steel strength, GPa | HE max strength, GPa | Ignition variable |
|----------------------|---------------------|----------------------|-------------------|
| 0.05                 | 0.5                 | 0.3                  | 20                |
| 0.2                  | 0.5                 | 0.3                  | 90                |
| 0.4                  | 0.5                 | 0.3                  | 200               |
| 0.6                  | 0.5                 | 0.3                  | 230               |
| 0.4                  | 0.3                 | 0.3                  | 160               |
| 0.4                  | 0.5                 | 0.3                  | 370*              |
| 0.4                  | 0.5                 | 0.15                 | 220               |

The LLNL Steven test vehicle is similar to the AWE version, but has several important differences. The explosive disk is 110 mm in diameter, and the PTFE ring is 23 mm wide. Perhaps of more importance is that the back plate is permitted to flex under the impact, rather than being stiffly supported. Tests at LLNL with the same explosive gave a no-go at 100 m/s and an HEVR event at 110 m/s. Our simulations of the LLNL test at 110 m/s, using the same mesh size in the HE and test fixture that we used for the AWE test fixture, gave the same maximum ignition parameter and maximum specific surface area as the AWE test at 70 m/s. As illustrated in Figure 9, the peak pressure is a very poor choice for the ignition parameter. The

peak pressure occurs in the middle of the HE on the axis of symmetry. Although both experiments ignited, the peak pressure in the LLNL Steven test is much less than that in the AWE version, even though it experiences a higher velocity projectile, principally due to the flexure permitted in the LLNL test.

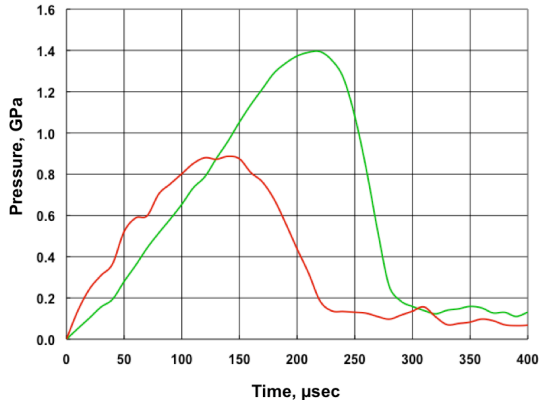


Fig. 9. Calculated pressure histories from AWE and LLNL Steven tests with ignition and subsequent burn suppressed. Green curve (peak value 1.4 GPa) is from the AWE test at 70 m/s. Red curve (peak value 0.9) is from the LLNL test at 110 m/s.

#### Calculations of the Burn After Ignition

We performed some initial calculations of the evolution of burn after ignition to examine the sensitivity of the results of porosity, ignition front velocity, confinement, and specific surface area.<sup>12</sup> For these calculations we assumed that a steel sphere (tensile strength 0.5 GPa) with 22 mm outside diameter and 20 mm inside diameter was uniformly filled with identical particles and ignited at the center. Due to the strong convergence of this idealized spherical geometry, the peak pressure at the ignition point is anomalously large and strongly dependent on the mesh size. Instead, we report the volume-averaged pressure for the entire sphere, which is not dependent on the mesh sizes we used. The nominal meshing used 30 elements across the diameter of the sphere.

For the baseline case of 500 μm diameter particles, the peak pressure, 0.2 GPa, was about twice the static failure pressure of the vessel. About 0.4 g of the 7 g of explosive fill burned. Increasing

the initial porosity of the explosive fill from 17% to 35% delayed the appearance of the peak pressure from 80 μs to 180 μs, and reduced the peak value although the mass burned was the same. Reducing the ignition front velocity from 300 m/s to 100 m/s delays the appearance of the peak pressure by about 40 μs. Increasing the confinement by doubling the steel strength doubled the peak pressure and doubled the mass burned. Decreasing the particle diameter from 500 μm to 50 μm doubled the peak pressure and increased the mass burned by seven-fold. A test article 200 mm diameter filled with 500 μm particles is a geometrically scaled version of the original size test vehicle with 50 μm particles. As a result, the 7 kg explosive assembly of 500 μm particles releases the energy of 2.8 kg of explosive. These results illustrate the increased hazard associated with large amounts of explosive damaged to the same degree.

#### Calculations with the Combined Model

We performed calculations of variants of the Steven test that included deformation, ignition, and burn. In our axisymmetric simulations without burn, the projectile rebounds from the test assembly with a coefficient of restitution approximately equal to 0.2. For our simulations with burn, the cover plate drives the projectile back with a velocity approximately equal to the impact velocity. As a result, the inertia of the projectile provides substantial confinement. We demonstrated this by artificially removing the projectile at various times after ignition. The mass burned as a function of time is shown in Figure 10. The absolute value of the mass burned in that figure is probably too small, based on our assessment of the mass burned as inferred from the measured air blast overpressure. The mass burned depends largely on the specific surface area, which has not been independently calibrated. We are confident, however, that our simulations illustrate the dependence of violence measured (for example the air blast) on circumstances of the experiment.

To further assess the influence of confinement, we designed a test vehicle that exaggerates the annular clearance between the projectile radius and the strong ring. The clearance in the AWE design is 20 mm; the clearance for the LLNL design is 45 mm. In our exaggerated design, the

clearance is 70 mm. For that design, using a rigid backing, the ignition criterion is met with a projectile velocity of 55 m/s. Despite having nearly 8 times the explosive mass in the test vehicle compared with the AWE design, the mass burned, and hence the violence is less than half. In contrast to the conditions of the 7 kg computational test design for burn after ignition as described above, the volume of damaged explosive is controlled by the projectile diameter, not the HE diameter, and the confinement is much reduced.

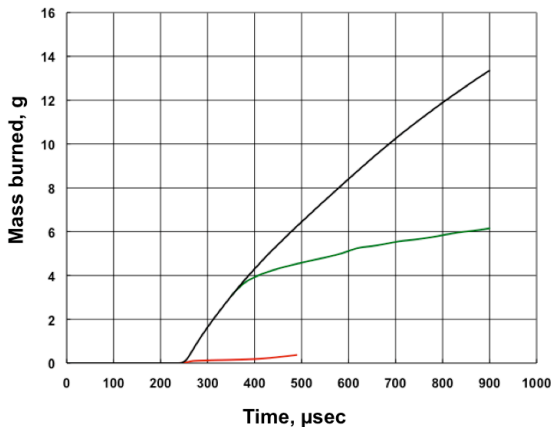


Fig. 10. Mass burned as a function of time (from top to bottom) when the projectile remains in contact, when the projectile is removed 150  $\mu$ s after ignition, and when the projectile is removed just after ignition.

### Acknowledgements

The work presented here was the result of a two-year secondment of one of us (JER) to the laboratory of the other (AGJ). Funding for this secondment came from three LLNL programs managed by Larry Fried, Alan Ross, Ron Streit, the Joint DoD/DOE Munitions Technology Development Program led at LLNL by Bruce Watkins, and also from three AWE activities led by Andy Abbott, Rod Drake, and Caroline Handley. Thanks are due to Jon Maienschein and Randy Simpson, LLNL, and to Keith Fleming and Hugh James, AWE, who supported the secondment from the early planning stages. Thanks are due to Ben Applin, Simon Chetwynd, Bob Hughes, Gurdip Kalsi, Brian Lambourn, Dave Watkins, and Nick Whit-

worth from AWE for technical support and also for helping to make a foreigner feel welcomed. Thanks are also due to Kristine Ramirez and Sue Stacy, LLNL, for administrative support that reached across the Atlantic. Finally, thanks and apologies from JER are due to the many others who have not been mentioned here.

### References

1. JW Kury, E James, BM Dobratz, M Finger, LG Green, EL Lee, and RR Mcguire, "Explosive testing at the Lawrence Livermore Laboratory -- Philosophy and practice," LLNL report UCRL-79391, June 1977.
2. AJ Clear, "Standard laboratory procedures for sensitivity and stability of explosives, Picatinny Arsenal Report 1401, Revision 1, February 1950.
3. LR Simpson, MF Foltz, "LLNL small-scale drop-hammer impact sensitivity test," LLNL report UCRL-ID-119665, January 1995.
4. GR Walker, ed. "Manual of sensitiveness tests," TTCP panel G-2 (Explosives), Working group on Sensitiveness, Canadian Armament R&D Establishment, 1966.
5. AS Dyer and JW Taylor, "Initiation of detonation by friction on a high explosive charge," 5<sup>th</sup> Symp. (Int.) on Detonation, Pasadena CA, 1970, p291.
6. LG Green and GD Dorough, "Further studies on the ignition of explosives," 4<sup>th</sup> Detonation Symp. (Int.), Silver Spring, MD, 1965, p479.
7. SK Chidester, LG Green, CG Lee, "A frictional work predictive method for the initiation of solid high explosives from low pressure impacts," 10<sup>th</sup> Detonation Symp. (Int.), Boston MA, 1993, p785.
8. S Wortley, AG Jones, J Allum, "Low speed impact of pristine and aged solid high explosive," 12<sup>th</sup> Detonation Symp. (Int.), San Diego, CA, 2002.
9. DJ Idar, RA Lucht, JW Straight, RJ Scammon, RV Browning, J Middleditch, JK Dienes, CB Skidmore, and GA Buntain, "Low amplitude insult project: PBX 9501 high explosive violent reaction experiments," 11<sup>th</sup> Detonation Symp. (Int.), Snowmass, CO, 1998, p101.
10. AG Jones, AJ Dale, CT Hughes and M Cartwright, "Low velocity impacts on explosive assemblies," 13<sup>th</sup> Detonation Symp. (Int.), Norfolk, VA, 2006, p700.

11. JE Reaugh, "Progress in model development to quantify High Explosive Violent Response (HEVR) to mechanical insult," LLNL report LLNL-TR-405903, August 2008.
12. JE Reaugh, "Calculating the dynamics of high explosive violent response (HEVR) after ignition," LLNL report LLNL-TR-407915, October 2008.
13. JE Reaugh, Implementation of strength and burn models for plastic-bonded explosives and propellants," LLNL report LLNL-TR-412938, May 2009.
14. JE Reaugh, "Implementation of an interactive model for HEVR," LLNL report, in process.
15. OYu Vorobiev, BT Liu, IN Lomov, TH Antoun, "Simulation of penetration into porous geologic media," *Int. J. Impact Engineering*, **34**, April 2007, p721.
16. C Gruau, D Picart, R Belmas, E Bouton, F Delmair-Sizes, J Sabatier, H Trumel, "Ignition of a confined high explosive under low velocity impact," *Int. J. Impact Engineering*, **36**, 2009, p537.
17. *LS-DYNA Keyword users manual*, Livermore Software Technology Company (LSTC), Livermore, CA, May 2007, Version 971.
18. AI Atwood, KP Ford, DT Bui, PO Curran, TM Lyle, "Assessment of mechanically induced damage in solid energetic materials," *7<sup>th</sup> Int. Symp. On Special Topics in Chemical Propulsion*, Kyoto, Japan, September 2007.
19. JM Maienschein, JE Reaugh, and EL Lee, "Propellant impact risk assessment team report: PERMS model to describe propellant energetic response to mechanical stimuli," LLNL report. UCRL-ID-130077, February 1998.
20. AM Niles, F Garcia, DW Greenwood, JW Forbes, CM Tarver, SK Chidester, RG Garza, and LL Switzer, "Measurement of low level explosives reaction in gauged multi-dimensional Steven impact tests," *Shock Compression of Condensed Matter - 2001*, 2002, p886.
21. MR Baer, JW Nunziato, "A two-phase mixture theory for the deflagration-to-detonation transition (DDT) in reactive granular materials," *Int. J. Multiphase Flow*, **12** (6) 1986, p861.
22. AK Lapela, R Menikoff, JD Bdzil, SF Son, DS Stewart, "Two-phase modeling of deflagration-to-detonation transition in granular materials: Reduced equations," *Phys. Fluids*, **13** (10) 2001, p3002.
23. JE Reaugh and EL Lee, "Isochoric burn, an internally consistent method for the reactant to product transformation in reactive flow," *12<sup>th</sup> Detonation Symp. (Int.)*, San Diego, CA, 2002.
24. EL Lee, HC Hornig, "Equation of state of detonation product gases," UCRL-70809, *12<sup>th</sup> Int. Symp. on Combustion*, Potier, France, 1968.
25. LE Fried, WM Howard, PC Souers, "EXP6: A new equation of state library for high-pressure thermochemistry," *12<sup>th</sup> Detonation Symp. (Int.)*, San Diego, CA, 2002.
26. S Bastea, K Glaesmann, and LE Fried, "Equations of state for high explosive detonation products with explicit polar and ionic species," *13<sup>th</sup> Detonation Symp. (Int.)*, Norfolk, VA, 2006.
27. JE Reaugh, "Computer simulations to study the explosive consolidation of powders into rods," *J. Appl. Phys.*, **61** (3) 1987, p962.
28. R Behrens, S Maharrey, "Chemical and Physical Processes that Control the Thermal Decomposition of RDX and HMX." In *Combustion of Energetic Materials*, KK Kuo, LT DeLuca, eds. Bege House: New York, 2002, p3
29. DM Williamson, CR Siviour, WG Proud, SJP Palmer, R Govier, K Ellis, P Blackwell, and C Leppard, "Temperature-time response of a polymer bonded explosive in compression," *J. Phys. D: Appl. Phys.* **41**, 085404, 2008.
30. DR Drodge, SJP Palmer, DM Williamson, WG Proud, and JE Field, "2<sup>nd</sup> Quarterly Report 2007, Mechanical and Microstructural Properties of Polymer Bonded Explosives, April 2007
31. DA Wiegand, B Reddingius, K Ellis, and C Leppard, "Mechanical failure properties of a polymer composite as a function of hydrostatic pressure," (to be published), *J. Mechanics and Physics of Solids*, 2010.
32. DM Hoffman and JB Chandler, "Aspects of the Tribology of the Plastic Bonded Explosive LX-04," *Propellants, Explosives, Pyrotechnics*, **29**, 2004, p368.

This work performed under the auspices of the U.S. Department of Energy by Lawrence Livermore National Laboratory under Contract DE-AC52-07NA27344.